Future prospects of α_s from NNLO jets at the LHC and beyond

Joao Pires[1,2]

[1]Università degli Studi di Milano, Milano, Italy
[2]Max-Planck-Institut for Physics, München, Germany

Abstract: The extraction of the strong coupling α_s using inclusive jet production in proton-proton collisions is reviewed, including upcoming NNLO theoretical developments.

The measurement of inclusive jet production in proton-proton collisions is an important part of the physics program at the LHC, where these measurements can provide a precise determination of the strong coupling constant at the highest possible energy scales and also be used to obtain information about the structure of the proton. For this observable, the cross section has a simple and clean definition,

$$\frac{\mathrm{d}^2\sigma_{\mathrm{inc.jet}}}{\mathrm{d}p_{\mathrm{T}}\mathrm{d}y} = \frac{1}{\mathcal{L}}\frac{N_{\mathrm{jets}}}{\Delta p_T \Delta_y} \tag{1}$$

where we count the number of observed jets within a given transverse momentum p_{T} and rapidity y interval per unity of integrated luminosity. The mechanism responsible for jet production at a hadron collider is the scattering at high-energy of the proton constituents, quarks and gluons, that produces a narrow spray (or jet) of colourless strongly interacting hadrons, clustered around the direction determined by the high-energy scattering event. The precise definition of a jet is then obtained with a jet algorithm, a procedure that performs a sequential recombination of the candidate jet constituents using the relative geometric distance $\Delta_R = \sqrt{\Delta\Phi^2 + \Delta y^2}$ (where Φ and y are their azimuthal angle and rapidity), to collect all the particles belonging to a specific jet, determining at the end of the procedure its properties, such as the jet four-momentum, p_{T} and rapidity. At the LHC, the jet algorithm of choice is the anti-k_T algorithm [1] with jet resolution parameters in the range $R = 0.4 \sim 0.7$. As an example we show in Fig. 1 the double differential inclusive jet cross section measurement by CMS [2] with a total integrated luminosity of 5 fb^{-1} from $\sqrt{s} = 7$ TeV pp collisions together with the experimental systematic uncertainties. We observe that the dominant systematic uncertainty comes from the jet energy scale uncertainty, estimated to be 2.0–2.5% [3]. Due to the steep slope of the p_{T} spectrum, this translates into a $< 10\%$ uncertainty on the cross section measurement, opening the possibility to do precision tests of QCD and ultimately α_s extractions from jet data using predictions from perturbative QCD.

perturbative QCD accuracy	$\frac{\mathrm{d}^2\sigma_{incl.jet}}{dp_{\mathrm{T}}d_y} \propto \alpha_s^2$	$R_{32} = \frac{\mathrm{d}\sigma_{3jet/2jet}}{d\overline{p}_{T_{1,2}}} \propto \alpha_s$	$\frac{\mathrm{d}^2\sigma_{3jet}}{dm_{jjj}dy_{max}} \propto \alpha_s^3$
NLO	✓[4,5,6]	✓[6]	✓[6]
NNLO	(partial)[7]	×	×

Table 1: Three observables to extract α_s from LHC jet data: the double differential inclusive jet cross section, the three-jet to two-jet cross section ratio differential in the average p_{T} of the two leading jets and the three jet double-differential cross section in the three jet mass and maximum rapidity of the three jet system. The references correspond to the state of the art of the corresponding theory prediction.

In Table 1 we summarise the observables that have been proposed to extract α_s with jet data from the LHC together with the state of the art accuracy in the theory prediction from perturbative

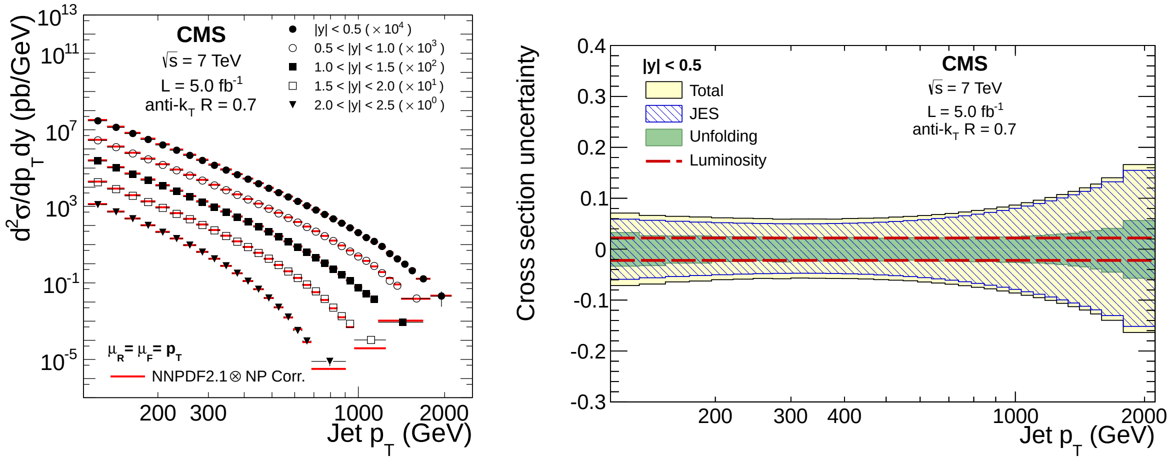

Figure 1: Inclusive jet cross sections (left) for five different rapidity bins, for data (markers) and theory (thick lines) using the NNPDF2.1 PDF set and relative experimental uncertainties (right) of the inclusive jet measurement [2].

QCD. For the remainder of this contribution we will concentrate on the double differential inclusive jet cross section.

In reference [8] a first α_s extraction from this observable was performed using 37 pb^{-1} of data recorded by the ATLAS detector from pp collisions at $\sqrt{s} = 7$ TeV [9]. In this study, 42 data points of the double differential inclusive jet cross section in the p_T range 45 GeV to 600 GeV together with their statistical and systematic uncertainties and their correlation were used, and the respective $\alpha_\mathrm{s}(M_Z)$ obtained values are shown in Fig. 2. Theoretical predictions for the inclusive jet cross sections are calculated in perturbative QCD at next-to-leading order (NLO) corrected by non-perturbative contributions to obtain the prediction at the particle level. The final result of the fit reads [8],

$$\begin{aligned}\alpha_\mathrm{s}(M_Z) \quad = \quad & 0.1151 \pm 0.0001 \text{ (stat.)} \pm 0.0047 \text{ (exp. syst.)} \pm 0.0014 \text{ (p}_\mathrm{T}\text{ range)} \\ & \pm 0.0060 \text{ (jet size)}^{+0.0044}_{-0.0011} \text{ (scale)}^{+0.0022}_{-0.0015} \text{ (PDF choice)} \\ & \pm 0.0010 \text{ (PDF eig.)}^{+0.0009}_{-0.0034} \text{ (NP corrections)},\end{aligned} \qquad (2)$$

where the dominant systematic uncertainty arises in the difference between the results obtained with jet sizes $R = 0.4$ and $R = 0.6$ followed by experimental systematics (dominated by the jet energy scale) and the scale uncertainty of the perturbative prediction.

More recently, the CMS collaboration presented in [10] an α_s extraction based on the full 5 fb^{-1} $\sqrt{s} = 7$ TeV dataset [2], using 133 data points in the p_T range 114 GeV to 2116 GeV of the inclusive jet cross section with jet size $R = 0.7$. In Table 2 the obtained α_s values in bins of rapidity up to $|y| < 2.5$ are shown [10]. Using all rapidity bins the strong coupling constant has been determined to be [10],

$$\alpha_\mathrm{s}(M_Z) = 0.1185 \pm 0.0019\,(\mathrm{exp}) \pm 0.0028\,(\mathrm{PDF}) \pm 0.0004\,(\mathrm{NP})\,^{+0.0053}_{-0.0024}\,(\mathrm{scale}),$$

where the scale uncertainty of the NLO QCD prediction dominates the total uncertainty in the α_s value followed by the PDF uncertainty.

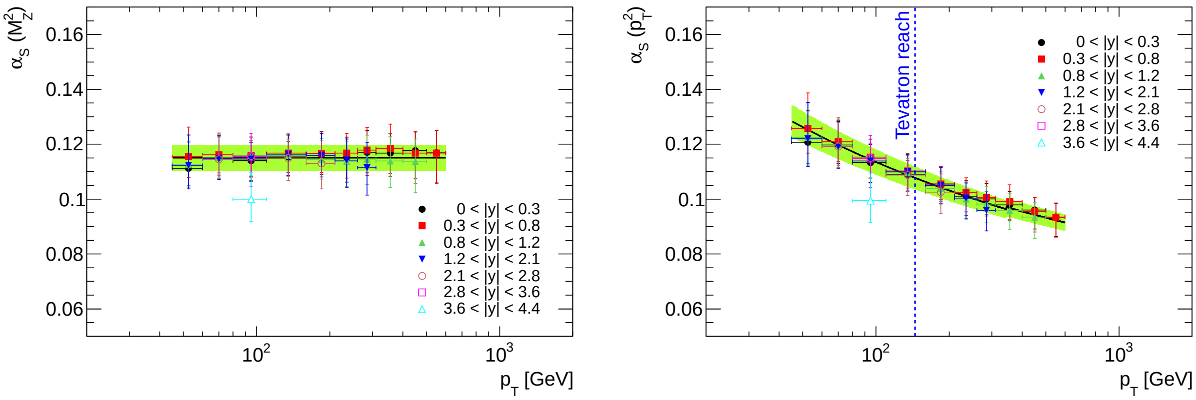

Figure 2: Global weighted $\alpha_s(M_Z^2)$ (left) and evolved to the corresponding p_T scale (right) averages (green bands) together with the α_s values (with asymmetric uncertainties) obtained in all the (p_T; $|y|$) bins used in the combination. The blue vertical line indicates the highest p_T value used in the Tevatron $\alpha_s(M_Z^2)$ determination, from the inclusive jet cross section [8].

While both determinations above are consistent within uncertainties with the world average value of $\alpha_s(M_Z) = 0.1185 \pm 0.0006$ [11], it is clear that the current theory uncertainties limit the achievable precision. The theoretical prediction may be improved by including the next-to-next-to-leading order (NNLO) perturbative predictions. This has the effect of (a) reducing the renormalisation and factorization scale dependence of the prediction and (b) improving the matching of the parton level theoretical jet algorithm with the hadron level experimental jet algorithm because the jet structure can be modeled by the presence of a third parton, directly addressing the currently dominant systematic uncertainties on the α_s determinations above.

$\|y\|_{\mathrm{range}}$	No. of data points	$\alpha_s(M_Z)$	χ^2/n_{dof}
$\|y\| < 0.5$	33	$0.1189 \pm 0.0024\,(\mathrm{exp}) \pm 0.0030\,(\mathrm{PDF}) \pm 0.0008\,(\mathrm{NP})^{+0.0045}_{-0.0027}\,(\mathrm{scale})$	16.2/32
$0.5 \leq \|y\| < 1.0$	30	$0.1182 \pm 0.0024\,(\mathrm{exp}) \pm 0.0029\,(\mathrm{PDF}) \pm 0.0008\,(\mathrm{NP})^{+0.0050}_{-0.0025}\,(\mathrm{scale})$	25.4/29
$1.0 \leq \|y\| < 1.5$	27	$0.1165 \pm 0.0027\,(\mathrm{exp}) \pm 0.0024\,(\mathrm{PDF}) \pm 0.0008\,(\mathrm{NP})^{+0.0043}_{-0.0020}\,(\mathrm{scale})$	9.5/26
$1.5 \leq \|y\| < 2.0$	24	$0.1146 \pm 0.0035\,(\mathrm{exp}) \pm 0.0031\,(\mathrm{PDF}) \pm 0.0013\,(\mathrm{NP})^{+0.0037}_{-0.0020}\,(\mathrm{scale})$	20.2/23
$2.0 \leq \|y\| < 2.5$	19	$0.1161 \pm 0.0045\,(\mathrm{exp}) \pm 0.0054\,(\mathrm{PDF}) \pm 0.0015\,(\mathrm{NP})^{+0.0034}_{-0.0032}\,(\mathrm{scale})$	12.6/18
$\|y\| < 2.5$	133	$0.1185 \pm 0.0019\,(\mathrm{exp}) \pm 0.0028\,(\mathrm{PDF}) \pm 0.0004\,(\mathrm{NP})^{+0.0053}_{-0.0024}\,(\mathrm{scale})$	104.1/132

Table 2: Determination of $\alpha_s(M_Z)$ in bins of rapidity using the CT10-NLO PDF set. The last row presents the result of a simultaneous fit in all rapidity bins [10].

In order to perform this computation one needs to systematically combine all radiative corrections to the perturbative cross section at the second order in the strong coupling. This includes the six parton tree-level, five-parton one-loop and four-parton two-loop matrix elements for parton-

parton scattering in QCD. For the partonic subprocess of pure gluon scattering this was achieved in [7], making use of the antenna subtraction scheme [12] to perform the analytic cancellation of IR singularities between real and virtual corrections at NNLO [13]. For hadron collider observables this includes contributions due to radiative corrections from partons in the initial state [14]. In this calculation, the QCD matrix elements are included in a parton-level generator NNLOJET, in development for the calculation of dijet production at NNLO in QCD, which integrates them over the exact full phase space to compute any infrared safe two-jet observable to NNLO accuracy.

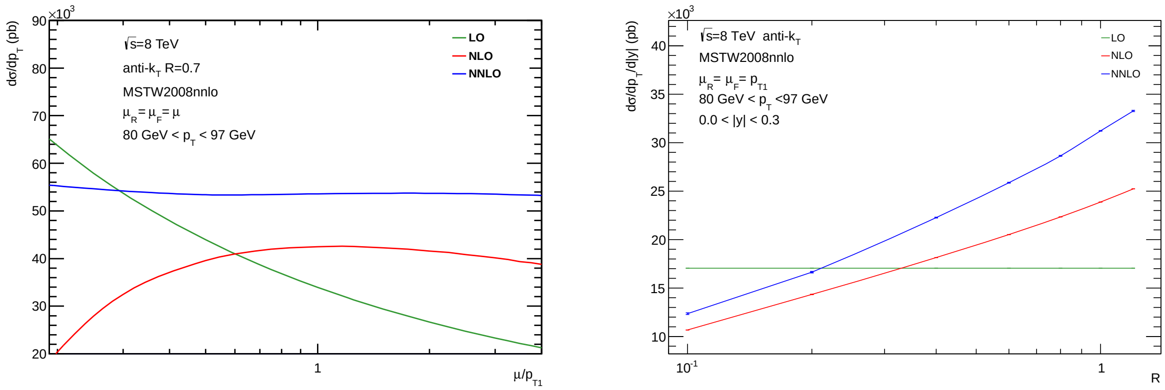

Figure 3: Scale dependence (left) and jet size parameter R dependence (right) of the inclusive jet cross section for the pure gluonic scattering subprocess at each order in perturbation theory, for 80 GeV $< p_{\mathrm{T}} <$ 97 GeV jet production with the anti-k_T algorithm and $\sqrt{s} = 8$ TeV [7].

In Fig. 3 we plot the results of this exercise where we show the perturbative predictions up to NNLO in QCD for jet production [7]. We stress that the predictions plotted for each order in the perturbative expansion contain only the pure gluonic scattering subprocess, and also in this example the central scale choice used to obtain the perturbative prediction was set to $\mu_R = \mu_F = p_{T1}$ (the p_{T} of the leading jet), with the MSTW2008NNLO PDF set fixed including for the evaluation of the LO and NLO contributions. We can observe that simultaneous variations of the factorisation and renormalisation scales at NNLO result in a rapidity integrated inclusive jet cross section with a flat scale dependence. Moreover we show the size of the NNLO corrections as a function of the jet size R, with the aim of addressing the currently dominant systematic uncertainties in α_{s} extractions from jet cross section measurements at the LHC.

In order for these improvements to materialise in future extractions of α_{s} from NNLO jets at the LHC, all the partonic subprocesses that contribute at NNLO are being added to the partial results in reference [7], to analyse data from Run II of the LHC. It is anticipated that these theoretical developments will contribute to reduce current theoretical uncertainties, namely the uncertainty from missing higher orders, the description of the perturbative cross section for different jet sizes and the perturbative prediction scale uncertainty.

References

[1] M. Cacciari, G. P. Salam and G. Soyez, JHEP **0804** (2008) 063 [arXiv:0802.1189 [hep-ph]].

[2] S. Chatrchyan *et al.* [CMS Collab.], Phys. Rev. D **87** (2013) 11, 112002 [Phys. Rev. D **87** (2013) 11, 119902] [arXiv:1212.6660 [hep-ex]].

[3] [CMS Collab.], CMS-DP-2012-006, CERN-CMS-DP-2012-006.

[4] S. D. Ellis, Z. Kunszt and D. E. Soper, Phys. Rev. Lett. **69** (1992) 1496.

[5] W. T. Giele, E. W. N. Glover and D. A. Kosower, Phys. Rev. Lett. **73** (1994) 2019 [hep-ph/9403347].

[6] Z. Nagy, Phys. Rev. Lett. **88** (2002) 122003 [hep-ph/0110315]; Z. Nagy, Phys. Rev. D **68** (2003) 094002 [hep-ph/0307268]

[7] A. Gehrmann-De Ridder, T. Gehrmann, E. W. N. Glover and J. Pires, Phys. Rev. Lett. **110** (2013) 16, 162003 [arXiv:1301.7310 [hep-ph]].; J. Currie, A. Gehrmann-De Ridder, E. W. N. Glover and J. Pires, JHEP **1401** (2014) 110 [arXiv:1310.3993 [hep-ph]].

[8] B. Malaescu and P. Starovoitov, Eur. Phys. J. C **72** (2012) 2041 [arXiv:1203.5416 [hep-ph]].

[9] G. Aad *et al.* [ATLAS Collab.], Phys. Rev. D **86** (2012) 014022 [arXiv:1112.6297 [hep-ex]].

[10] V. Khachatryan *et al.* [CMS Collab.], Eur. Phys. J. C **75** (2015) 6, 288 [arXiv:1410.6765 [hep-ex]].

[11] K. A. Olive *et al.* [PDG Collab.], Chin. Phys. C **38** (2014) 090001.

[12] A. Gehrmann-De Ridder, T. Gehrmann and E. W. N. Glover, JHEP **0509** (2005) 056 [hep-ph/0505111].

[13] E. W. Nigel Glover and J. Pires, JHEP **1006** (2010) 096 [arXiv:1003.2824 [hep-ph]]; A. Gehrmann-De Ridder, E. W. N. Glover and J. Pires, JHEP **1202** (2012) 141 [arXiv:1112.3613 [hep-ph]]; A. Gehrmann-De Ridder, T. Gehrmann, E. W. N. Glover and J. Pires, JHEP **1302** (2013) 026 [arXiv:1211.2710 [hep-ph]]; J. Currie, E. W. N. Glover and S. Wells, JHEP **1304** (2013) 066 [arXiv:1301.4693 [hep-ph]].

[14] A. Daleo, T. Gehrmann and D. Maitre, JHEP **0704** (2007) 016 [hep-ph/0612257]; A. Daleo, A. Gehrmann-De Ridder, T. Gehrmann and G. Luisoni, JHEP **1001** (2010) 118 [arXiv:0912.0374 [hep-ph]]; R. Boughezal, A. Gehrmann-De Ridder and M. Ritzmann, JHEP **1102** (2011) 098 [arXiv:1011.6631 [hep-ph]]; T. Gehrmann and P. F. Monni, JHEP **1112** (2011) 049 [arXiv:1107.4037 [hep-ph]]; A. Gehrmann-De Ridder, T. Gehrmann and M. Ritzmann, JHEP **1210** (2012) 047 [arXiv:1207.5779 [hep-ph]].